Volume 9 | Number 16 | 21 August 2022

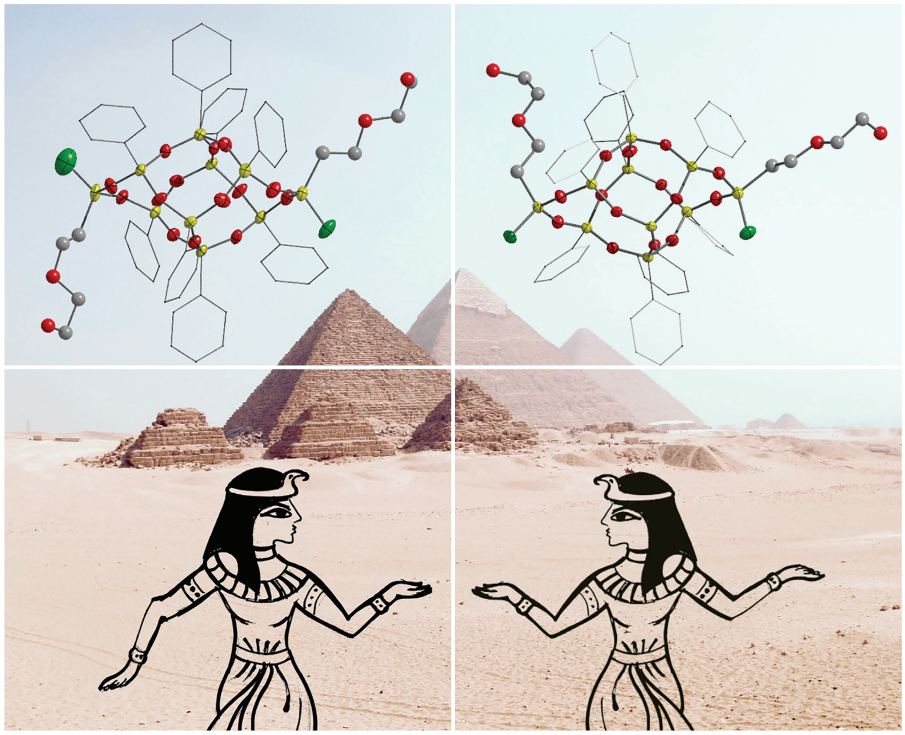

INORGANIC CHEMISTRY

FRONTIERS

CCS 中国化学会 CHINESE CHEMICAL SOCIETY

PEKING UNIVERSITY 1898

ROYAL SOCIETY OF CHEMISTRY

rsc.li/frontiers-inorganic

INORGANIC CHEMISTRY
FRONTIERS

RESEARCH ARTICLE

View Article Online
View Journal | View Issue

Cite this: *Inorg. Chem. Front.*, 2022, **9**, 3999

Hydroxyalkyl-substituted double-decker silsesquioxanes: effective separation of *cis* and *trans* isomers†

Anna Władyczyn,[a] Anna Gągor,[b] Katarzyna Ślepokura[a] and Łukasz John *[a]

In this work, we report the preparation, isolation, and characterization of a family of double-decker silsesquioxane architectures starting from the previously reported DDSQ-Me_2H_2 precursor, a mixture of *cis* and *trans* isomers. Using such a starting material results in a subsequent mixture of isomers when hydrosilylation reactions using DDSQ-Me_2H_2 and hydroxyalkyl-substituted alkenes catalyzed by Karstedt catalyst are performed. We describe a procedure to sequentially crystallize the two isomers from one another, affording a protocol potentially applicable to other closely related derivatives. The ability to access pure *cis* and *trans* isomers of double-decker silsesquioxanes may result in the preparation of new materials and polymers with well-defined properties. All resulting silsesquioxanes were characterized by multinuclear (^{1}H, ^{13}C, and ^{29}Si) NMR spectroscopy, FT-IR, and HR-MS. Additionally, we report five crystal structures of geometrical isomers, including two *cis* forms described in the literature for the first time. This is a breakthrough in itself and sets a new strategy for obtaining such exiting organosilicon-based systems.

Received 17th March 2022,
Accepted 10th May 2022

DOI: 10.1039/d2qi00577h

rsc.li/frontiers-inorganic

1. Introduction

Double-decker silsesquioxanes (DDSQs) occupy an indisputable place among the group of functionalized siloxane-based compounds. They throw light on the development of molecular and macromolecular organosilicon chemistry concepts.[1] This attractive group of silicon-containing species has been extensively studied due to their outstanding physicochemical properties. Double-decker silsesquioxanes have shown excellent potential for various applications, including such intriguing areas as materials engineering, smart and self-healing polymers, coordination chemistry, catalysis, and others.[2–19] The structure of a typical double-decker silsesquioxane is different from that of the symmetric cubic T_8 polyhedral oligomeric silsesquioxanes (POSSs). It constitutes an open cage network including two connected, *via* oxygen bridges, decks of cyclosiloxane rings located on top of one another with eight phenyl groups attached to Si atoms (Fig. 1).[20] This group of silsesquioxanes includes the two following structures: an open (Fig. 1, C) architecture and a closed framework (Fig. 1, A and B with one and two reactive group(s) on each lateral arm, respectively). Difunctional double-decker silsesquioxanes (Fig. 1, A) are routinely obtained as isomer mixtures, with geometric *cis* and *trans* isomer formation corresponding to the different spatial arrangements of the labile functional groups and inert groups on the double-decker silsesquioxane core.

Among the broad palette of the functionalized double-decker silsesquioxanes, several articles are devoted to forming a mixture containing *cis* and *trans* geometrical isomers in the case of difunctionalized silsesquioxane (Fig. 1, A) derivatives.[21–23] This limits the number of available pure crystalline double-decker silsesquioxane reactive monomers. Unfortunately, these isomers, regardless of the nature of the external organic arms, have identical or similar retention times during chromatographic purification, which makes them difficult to separate. The identical drawback is also observed in polyhedral oligomeric silsesquioxanes chemistry. For instance, Laine *et al.* pointed out that molecules containing different numbers of phenyl substituents exhibited the same R_f values.[24] Even though the distinction may seem unnoticed, it is worth noticing that polyhedral oligomeric silsesquioxane species can be regarded as oligomers rather than discrete molecular compounds.[25] This is one of the reasons for looking for non-chromatographic separation methods.

Since polyhedral oligomeric silsesquioxane species can be regarded as oligomers, scientists have become inspired to find more or less effective synthetic approaches for novel di-substi-

[a]*Faculty of Chemistry, University of Wrocław, 14 F. Joliot-Curie, 50-383 Wrocław, Poland. E-mail: lukasz.john@uwr.edu.pl*
[b]*Institute of Low Temperature and Structure Research, Polish Academy of Sciences, 2 Okólna, 50-422 Wrocław, Poland*

† Electronic supplementary information (ESI) available: ^{1}H, ^{13}C, ^{29}Si NMR, FT-IR, HR-MS spectra, X-ray crystallographic data, and dielectric studies. CCDC 2158320–2158323. For ESI and crystallographic data in CIF or other electronic format see DOI: https://doi.org/10.1039/d2qi00577h

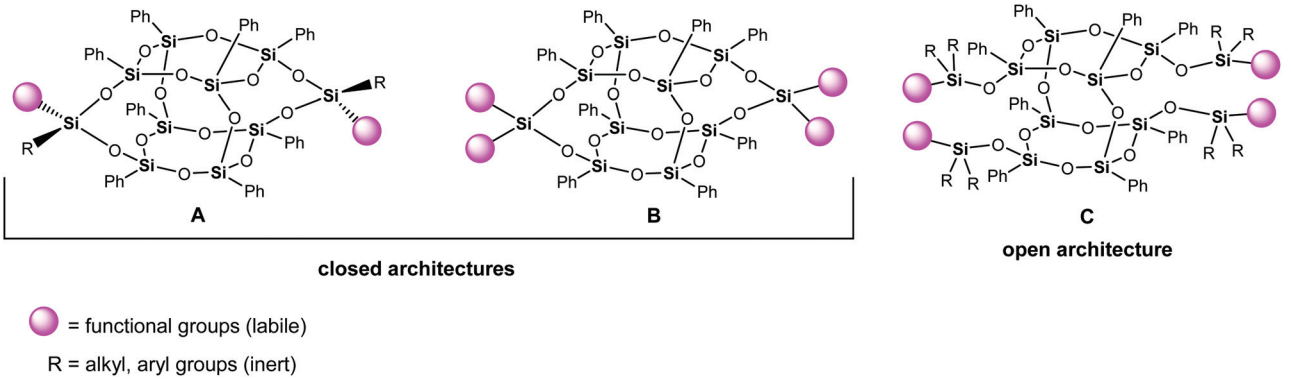

Fig. 1 Possible architectures of the double-decker silsesquioxanes.

tuted double-decker silsesquioxane monomers, including recrystallization, coprecipitation, formation of soluble coordination entities, and others. One of the attempts consists of coupling isobutyltrichlorosilane leading to the mixture of sodium salts. Unfortunately, only hydrolyzable *cis* and *trans* derivatives of closed double-decker silsesquioxanes were found; no further analysis was reported.[24]

Moreover, during this approach, other silsesquioxanes, except for the expected mixture of *cis* and *trans* isomers, such as mono-substituted cage-type polyhedral oligomeric silsesquioxane (T_7) and double-decker silsesquioxane with different substitution on lateral silicon atoms, are observed, which additionally complicates the reaction.[22] A similar strategy, based on the mixture of suitable sodium salts, led to diazido-functionalized double-decker silsesquioxane, obtained in the reaction of double-decker octasilsesquioxane-tetraol tetrasodium salt and (3-chloropropyl) methyldichlorosilane. Further azidation of the resulting dichloropropyl derivative gave an isomeric mixture of diazido double-decker silsesquioxane, not separable by column chromatography. Finally, careful recrystallization of the mixture solution was performed to obtain a pure crystalline *trans* isomer.[23] The above-mentioned examples show how difficult it is to separate a mixture of geometric isomers. If it is successful, this process requires long-term and often breakneck procedures that end with the separation of the *trans* isomer, with the *cis* isomer that remains in the mixture, and only due to the easier crystallization of a "more symmetrical" (center of symmetry in *trans* isomer) derivative.

A recent increase in the demand for well-defined and thermally stable systems has highlighted the importance of silsesquioxane-based architectures.[41–43] This paper describes a new approach to obtaining and separating *cis* and *trans* geometrical isomers of selected double-decker silsesquioxanes. More precisely, our interest was focused on various alkyl organic arms containing terminal hydroxy group(s) attached to double-decker silsesquioxane core, which have great potential in further modifications and formation of the hybrid building nano-blocks. We also report on crystal structures of *cis* isomers of the resulting double-decker silsesquioxanes. This is a breakthrough in itself and has never been done, according to our best knowledge.

2. Experimental

2.1. General procedures and chemicals

All the reactions and operations that required an inert atmosphere of N_2 or Ar were performed using a standard Schlenk apparatus and vacuum line techniques. Solvents for the synthesis: THF (tetrahydrofurane) and toluene; were purified using the Solvent Purification Systems (Inert, PureSolv EN 1–7 Base). Catalyst species were removed after reaction by filtration through Celite® 545 (Sigma-Aldrich) pad. Solvents for standard workup (methanol, hexane, acetone) were purchased from VWR International and ChemPur and were used as received. All the chemicals were obtained from commercial sources and used without further purification: TetraSilanolPhenyl POSS (Hybrid Plastics Inc.), dichloromethylsilane (>97% Sigma Aldrich), Karstedt catalyst (platinum(0)-1,3-divinyl-1,1,3,3-tetramethyldisiloxane complex solution) (in xylene, Pt ~ 2%, Sigma-Aldrich), ethylene glycol vinyl ether (97%, Sigma Aldrich), allyl alcohol (99%, Acros Organics), 3-allyloxy-1,2-propanediol (99%, Sigma-Aldrich), 4-allyl-2-methoxyphenol (99%, Sigma-Aldrich), triethylamine (Et_3N) (>99%, Sigma Aldrich).

2.2. Methods

^{1}H and ^{13}C NMR spectra were recorded with a Bruker Avance III 500 MHz spectrometer. ^{29}Si NMR spectra were recorded with a Bruker Avance III 600 MHz and a Bruker Avance III 500 MHz spectrometer. Chemical shifts are reported in parts per million (ppm) downfield from tetramethylsilane (TMS) and are referenced to residual peaks of deuterated NMR solvents. Chemical shift values for ^{29}Si{^{1}H} NMR spectra were referenced to TMS or DSS (2,2-dimethylsilapentane-5-sulphonate). Assignments are based on COSY and HSQC correlation experiments. Coupling constants (J) are reported in Hz. Standard abbreviations s, d, t, q, and m refer to singlet, doublet, triplet, quartet, and multiplet. High-resolution mass spectra were recorded using a Bruker apex ultra FTMS and Bruker microTOF-Q spectrometer using the electrospray technique. Elemental analyses (C, H, Si) were performed using a Vario EL III element analyzer (Hanau, Germany).

Single crystal X-ray diffraction data for *trans*-**1**, *trans*-**2**, *trans*-**3**, *cis*-**3**^{1} and *cis*-**3**^{2} crystals were collected on an Agilent

Technologies Gemini Ultra or Rigaku XtaLAB Synergy R, DW system at 100 K and 300 K. The data collection and processing utilized CrysAlis suite of programs. The structures were solved using direct methods (SHELXS97) and also using the dual-space algorithm (SHELXT program) and refined by full-matrix least-squares on F^2 (SHELXL program). Most of the non-hydrogen atoms were refined with anisotropic displacement parameters, and hydrogen atoms were placed at their calculated positions. For the details of disorder refinements, see the ESI.† Graphics were made using the Diamond 4.4.0 (Crystal Impact). Crystallographic data for the structural analysis has been deposited with the Cambridge Crystallographic Data Centre, no. 2158320–2158323† and 2158968. The complex dielectric permittivity, $\varepsilon^* = \varepsilon' - i\varepsilon''$, was measured between 80 and 300 K using an Agilent E4980A precision LCR meter in the frequency range of a 135 Hz–2 MHz. The overall experimental uncertainties were less than 5%. The dielectric experiment was performed on a polycrystalline sample in a pressed pellet with geometrical parameters (S = 20 mm^2, d = 0.5 mm). The silver electrodes were painted on both opposing faces.

2.3. Syntheses

2.3.1. Synthesis of DDSQ-Me$_2$H$_2$ (1). **1** was synthesized following the method reported by Morimoto *et al.*[26] with a slight modification. Typically, tetrahydroxyoctaphenyl double-decker silsesquioxane (DDSQ-(OH)$_4$) (10.00 g, 9.35 mmol), anhydrous THF (300 mL) and Et$_3$N (3.65 mL, 26.18 mmol) were added into a two-neck round-bottom flask equipped with a magnetic stirrer and stirred vigorously. The reaction mixture was placed in an ice-water bath and purged with nitrogen. Then methyldichlorosilane (5.90 mL, 56.80 mmol) was slowly added. The reaction mixture was allowed to warm to room temperature (RT), and was carried out for 24 hours. Then the mixture was filtered on a glass frit. Volatiles and THF were evaporated on the rotary evaporator. The crude product was recrystallized from methanol and filtered off. The white solid was dried *in vacuo*. The product was obtained with a yield of 86% (9.32 g, 8.08 mmol). ^{1}H NMR (500 MHz, CDCl$_3$), δ (ppm): 7.59–7.14 (m, –Ph, 40H), 4.98 (q, J = 1.5 Hz, Si–*H*, 2H), 0.37 (d, J = 1.7 Hz, Si–C*H*$_3$, 6H). ^{13}C NMR (126 MHz, CDCl$_3$) δ (ppm): 134.23–127.65 (–Ph), 0.65 (Si–*C*H$_3$). ^{29}Si NMR (119 MHz, CDCl$_3$) (*cis*/*trans* mixture), δ (ppm): −32.30 (Si–CH$_3$), −77.30 (*Si*–O–Si–Ph), −78.59 (*Si*–O–Si–Ph), −78.79 (Si–O–*Si*–Ph), −78.99 (Si–O–*Si*–Ph). FT-IR (KBr, ν_{max}/cm^{-1}): 3073, 3027 (C–H$_{Ar}$), 2966, 2923 (C–H$_R$), 2175 (Si–H), 1595 (C=C$_{Ar}$), 1431 (Si–CH$_3$), 1133 (br, Si–O–Si). HRMS (ESI$^+$, TOF/CH$_3$Cl): m/z: 1175.06 {calcd for [M + Na]$^+$ 1175.06}. Elemental analyses calcd for C$_{50}$H$_{48}$O$_{14}$Si$_{10}$: C, 52.05; H, 4.19; Si, 24.34; found C 52.06; H 4.18; Si, 24.36.

2.3.2. Synthesis of DDSQ-Me$_2$(hydroxypropyl)$_2$ (2). A three-neck round-bottom flask equipped with a magnetic stirrer and reflux condenser was flashed by pure dinitrogen, and charged with **1** (3.0 g, 2.60 mmol) and anhydrous toluene (200 mL). The mixture was stirred and heated to 70 °C. After the substrate was dissolved entirely, the Karstedt catalyst (10 µl, 0.448 µmol) was added. After stirring for 30 min, the allyl alcohol (0.88 ml, 0.76 g, 13.00 mmol) was added, and the mixture was heated up to 95 °C. The reaction was continuously stirred and heated for 24 h, after which it was cooled to RT. The solution was passed through a pad of Celite and concentrated on a rotary evaporator. *Separation*: the precipitate (0.9 g, pure *trans*-isomer) was crystallized from methanol (100 mL) (during a night in a refrigerator), filtered, and dried *in vacuo*. The filtrate was concentrated on a rotary evaporator giving yellow oil. The precipitate (2.5 g, mixture of *cis* and *trans*-isomer) was crystallized from hexane (100 mL). White solid (2.1 g, pure *trans*-isomer) was separated by filtration and recrystallized from methanol (10 mL). The filtrate was concentrated, giving yellow oil. As proved by the ^{29}Si NMR spectrum, this fraction contains unreacted allyl alcohol (substrate) and *cis*-**2**. The total yield (considering only the pure *trans*-**2**) was 91% (3 g, 2.36 mmol). ^{1}H NMR (500 MHz, CDCl$_3$) δ (ppm): 7.61–7.02 (m, –*Ph*, 40H), 3.46 (td, J = 6.7, 1.7 Hz, Si–CH$_2$CH$_2$C*H*$_2$OH, 4H), 1.62 (m, Si–CH$_2$C*H*$_2$CH$_2$OH, 4H), 1.25–1.04 (m, Si–C*H*$_2$CH$_2$CH$_2$OH, 4H), 0.79–0.64 (s (br), Si–CH$_2$CH$_2$CH$_2$O*H*, 2H), 0.30 (s, Si–C*H*$_3$, 6H). ^{13}C NMR (126 MHz, CDCl$_3$) δ (ppm): 134.98, 134.96, 134.83, 132.86, 131.90, 131.37, 128.78, 128.64 (*Ph*), 66.04 (Si–CH$_2$CH$_2$*C*H$_2$OH), 26.99 (Si–CH$_2$*C*H$_2$CH$_2$OH), 13.46 (Si–*C*H$_2$CH$_2$CH$_2$OH), 0.0 (Si–*C*H$_3$). ^{29}Si NMR (119 MHz, CDCl$_3$) δ (ppm): *trans*-**2**: −17.41 (*Si*–CH$_3$), −78.59 (Si–O–*Si*–Ph), −79.56 (Si–O–*Si*–Ph); *cis*-**2**: −17.23 (*Si*–CH$_3$), −77.26 (Si–O–*Si*–Ph), −78.43 (Si–O–*Si*–Ph), −78.74 (Si–O–*Si*–Ph). FT-IR (KBr, ν_{max}/cm^{-1}): 3435 (OH, br), 3073, 3052, 3027 (C–H$_{Ar}$), 2933, 2876 (C–H$_R$), 1594 (C=C$_{Ar}$), 1431 (Si–CH$_3$), 1132 (br, Si–O–Si). HRMS (ESI$^+$, TOF/CH$_3$Cl): m/z: 1291.14 {calcd for [M + Na]$^+$ 1291.15}. Elemental analyses calcd for C$_{56}$H$_{60}$O$_{16}$Si$_{10}$: C, 52.96; H, 4.76; Si, 22.12; found C, 52.86; H 4.80; Si, 22.20.

2.3.3. Synthesis of DDSQ-Me$_2$(hydroxyethyloxyethyl)$_2$ (3). The synthesis of **3** proceeded analogically to that of **2**, but instead of allyl alcohol, glycol vinyl ether (1.17 mL, 1.15 g, 13 mmol) was used. The reaction mixture was continuously stirred and heated for 24 h, after which it was cooled to RT. The solution was passed through a pad of Celite and concentrated on a rotary evaporator. *Separation*: the precipitate (1.20 g, pure *trans*-isomer) was crystallized from methanol (100 mL) (during a night in a refrigerator), filtered, and dried *in vacuo*. The filtrate was concentrated on a rotary evaporator giving white oil. The precipitate (1.92 g, mixture of *cis*-**3** and *trans*-**3**) was crystallized from hexane (100 mL). The white solid was separated by filtration and recrystallized from acetone (10 mL), dried *in vacuo*, giving the white, crystalline product (1.80 g pure *trans*-**3**). The filtrate was concentrated, giving yellow oil. As proved by the ^{29}Si{H} NMR spectrum and crystal structure, this fraction contains unreacted ether substrate and *cis*-isomer. The total yield (considering only the pure *trans*-**3**) is 87% (3 g, 2.26 mmol). ^{1}H NMR (500 MHz, CDCl$_3$) δ (ppm): 7.54–7.13 (m, –Ph, 40H), 3.64–3.53 (m, Si–CH$_2$C*H*$_2$O, 4H), 3.48 (q, J = 4.5 Hz, OCH$_2$CH$_2$OH, 4H), 3.27–3.18 (m, –OCH$_2$CH$_2$OH, 4H), 1.69 (s, –O*H*, 2H), 1.21–1.11 (m, Si–C*H*$_2$CH$_2$O, 4H), 0.31 (s, Si–C*H*$_3$, 6H). ^{13}C NMR (126 MHz, CDCl$_3$) δ (ppm): 134.20, 134.05, 131.95, 131.03, 130.65, 128.03, 127.88, (*Ph*), 71.28 (OCH$_2$CH$_2$OH), 67.05 (Si–CH$_2$*C*H$_2$O), 61.89 (OCH$_2$*C*H$_2$OH),

18.92 (Si–CH_2CH_2O), −0.00 (Si–CH_3). ^{29}Si NMR (99 MHz, $CDCl_3$) δ (ppm): *cis*-**3**: −20.04 (*Si*–CH_3), −77.45 (*Si*–O–Si–Ph), −78.88 (Si–O–*Si*–Ph), −78.94, −79.26 (*Si*–O–Si–Ph); *trans*-**3**: −19.55 (*Si*–CH_3), −78.59 (*Si*–O–Si–Ph), −79.60 (Si–O–*Si*–Ph). FT-IR (KBr, ν_{max}/cm^{-1}): 3436 (OH, br), 3073, 3051 (C–H_{Ar}), 2925, 2855 (C–H_R), 1594 (C=C_{Ar}), 1461 (Si–CH_3), 1134 (br, Si–O–Si). HRMS (ESI^+, TOF/CH_3Cl): *m*/*z*: 1351.15 {calcd for $[M + Na]^+$ 1351.17}. Elemental analyses calcd for $C_{58}H_{64}O_{18}Si_{10}$ C, 52.38; H, 4.85; Si, 21.12; found C, 52.26; H, 4.92; Si, 21.08.

2.3.4. Synthesis of DDSQ-Me_2(2,3-dihydroxypropoxyethyl)$_2$ (4). The synthesis of **4** proceeded analogically to that of **2**, where instead of allyl alcohol, 3-allyloxy-1,2-propanediol (1.609 ml, 1.718 g, 13.00 mmol) was added. The reaction mixture was continuously stirred and heated for 24 h, after which it was cooled to RT. The solution was passed through a pad of Celite and concentrated on a rotary evaporator. *Separation*: the precipitate (1.3 g, pure *trans*-isomer) was crystallized from methanol (100 mL) (during a night in a refrigerator), filtered, and dried *in vacuo*. The filtrate was concentrated on a rotary evaporator giving white oil. Next, the precipitate (2.1 g, mixture of unreacted substrate, *cis*-**4**, and *trans*-**4**) was crystallized from hexane (100 mL). Grey solid was three times separated by filtration and recrystallized from methanol (10 mL) to remove the unreacted substrate. Finally, a white, crystalline precipitate was obtained (0.554 g, pure *trans*-isomer). The filtrate was concentrated, giving yellow oil. As proved by the ^{29}Si{H} NMR spectrum, this fraction contains unreacted 3-allyloxy-1,2-propanediol (substrate) and *cis*-**4**. The total yield (considering only the pure *trans*-**4**) is 72% (2.65 g, 1.87 mmol). ^{1}H NMR (500 MHz, $CDCl_3$) δ (ppm): 7.55–7.15 (m, –Ph, 40H), 3.65 (tt, J = 5.9, 3.9 Hz, –OCH_2CH(OH)CH_2, 2H), 3.52 (diastereotopic (7a) dd, J = 11.4, 3.9 Hz, –OCH_2CH(OH)CH_2OH, 2H), 3.47–3.40 (diastereotopic (7b) m, –OCH_2CH(OH)CH_2OH, 2H), 3.35–3.18 (m, Si–$CH_2CH_2CH_2OCH_2$, 8H), 2.47–1.84 (m, OCH_2CH(O*H*)CH_2OH, 2H), 1.70–1.61 (m, Si–$CH_2CH_2CH_2OCH_2$, 4H), 0.81–0.60 (m, Si–$CH_2CH_2CH_2OCH_2$, 4H), 0.30 (s, Si–CH_3, 6H). ^{13}C NMR (126 MHz, $CDCl_3$) δ (ppm): 134.93, 134.79, 132.80, 131.88, 131.34, 128.74, 128.61 (Ph), 74.54 (–OCH_2CH(OH)CH_2OH), 72.95 (–OCH_2CH(OH)CH_2OH), 71.23 (–OCH_2CH(OH)CH_2OH), 64.96 (Si–$CH_2CH_2CH_2OCH_2$), 23.67 (Si–$CH_2CH_2CH_2OCH_2$), 13.59 (Si–$CH_2CH_2CH_2OCH_2$), 0.0 (Si–CH_3). ^{29}Si NMR (99 MHz, $CDCl_3$) δ (ppm): *trans*-**4**: −17.52 (*Si*–CH_3), −78.64 (Si–O–*Si*–Ph), −79.57 (*Si*–O–Si–Ph); *cis*-**4**: −17.53 (*Si*–CH_3), −78.63 (Si–O–*Si*–Ph), −79.44 (*Si*–O–Si–Ph), −79.69 (Si–O–*Si*–Ph). FT-IR (KBr, ν_{max}/cm^{-1}): 3455 (OH, br), 3073, 3051, 3008 (C–H_{Ar}), 2960, 2929, 2860 (C–H_R), 1595 (C=C_{Ar}), 1431 (Si–CH_3), 1132 (br, Si–O–Si). HRMS (ESI^+, TOF/CH_3Cl): *m*/*z*: 1439.24 {calcd for $[M + Na]^+$ 1439.22}. Elemental analyses calcd for $C_{62}H_{72}O_{20}Si_{10}$: C, 52.51; H, 5.12; Si, 19.80; found C, 52.46; H 5.13; Si, 19.87.

3. Results and discussion

Following the latest literature reports on double-decker silsesquioxanes, it can be easily noted that in the case of difunctionalized double-decker silsesquioxane derivatives (Fig. 1, A), the authors describe the preparation of a mixture of geometric isomers. If a monocrystal is likely to be obtained, the *trans* form usually crystallizes, and the *cis* isomer remains in the mixture of the products, which is further difficult to separate. In the case of *cis* isomers, the number of crystal structures is negligible.[26,27–29] They constitute the examples in which the organic arms attached to the double-decker silsesquioxane core have aromatic groups that stabilize the side substituents, among other possible interactions, by π–π stacking. In turn, there are no reports on derivatives containing alkyl side groups. This inspired us to undertake research in an attempt to obtain well-defined *cis*-type isomers that would contain alkyl substituents possessing hydroxyl groups, which would be easy to modify in further reactions to obtain new nano-blocks for complex hybrid materials (Fig. 2).

Moreover, the selection of organic arms was also dictated by creating weak intermolecular interactions possibilities (*e.g.*, hydrogen bonds, hydrophobic interactions, π–π stacking, C–H···π interactions, *etc.*). The presence of weak interactions between phenyl substituents, sidearms, and solvent molecules in the crystal stabilize architectures formed in the solid state.

We considered DDSQ-Me_2H_2 (**1**) as a starting substrate to further modifications. This compound is routinely obtained in the reaction between DDSQ-$(OH)_4$ or its sodium salt and methyldichlorosilane.[30–32] However, it is commonly known that in most synthetic protocols, a significant excess of silane is used, and on the other hand, yields are around or even below 50%.

We slightly modified its synthesis, focusing on substrates' ratios and raising the yield, mixing substrates in a 1 : 6 molar ratio that resulted in 86% overall yield. The final product was characterized by NMR (^{1}H, ^{13}C, and ^{29}Si), FT-IR spectroscopy, and HR-MS spectrometry (see ESI, Fig. S1–S5†). The results state that the difunctional **1** was successfully obtained. ^{29}Si NMR spectrum (Fig. 3) indicates five signals (δ = −32.28, −77.30, −78.59, −78.79, and −78.99 ppm) which is expected for the mixture of isomers.[33] Although both isomers have the same chemical environment in the SiO_3Ph unit, it should not be excluded that their ^{29}Si resonance signals are not isochronous for isomers. It can also be found in the literature that

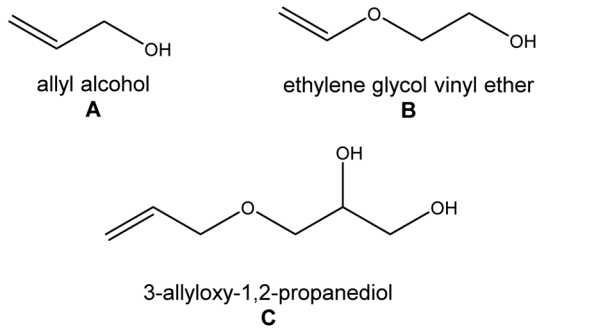

Fig. 2 Hydroxyalkyl-substituted alkenes used in hydrosilylation reactions.

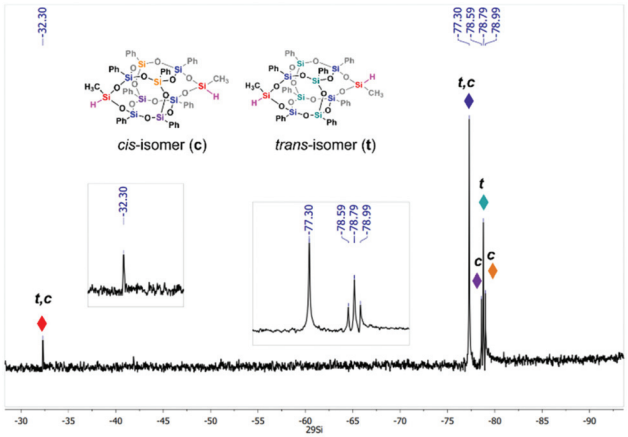

Fig. 3 ^{29}Si NMR spectrum of *cis*/*trans* mixture of **1**.

geometric isomerism influences the shifts of signals on the ^{29}Si NMR spectrum.[23,28,33,34]

Furthermore, the X-ray quality single crystals of *trans*-**1**·C_7H_8 were obtained from toluene saturated solution. As a result, the *trans*-**1** crystal structure was determined (see ESI, Table S1†). For this isomer, to date, only a crystal structure that does not form a solvate has been published.[33] Therefore, a valid justification here seems to be that the crystal structure obtained for *trans*-**1**·C_7H_8 is stabilized by a solvent molecule (toluene) in the crystal lattice by C–H···π interactions.[36] To confirm this, we also investigated the effect of the solvent in further extensions of **1** *via* hydrosilylation by modifying the lateral hydroxyalkyl arms. Our model shows that the structure has three conformers (depending on the arrangement of lateral Si atoms with methyl groups, Si–Me). Diffraction data analysis reveals that *trans*-**1**·C_7H_8 crystallizes in the triclinic space group $P\bar{1}$. There are two crystallographically independent molecules in a unit cell, both centrosymmetric. One of them is presented in Fig. 4A. Symptomatic value for the C–Si–Si–C pseudo-torsion angle (180°) indicates obtaining the *trans* isomer, but there is a disorder in the Si–Me group in both molecules. The double-decker silsesquioxane core, as presented in Fig. 4B, arranges itself in three positions that differ in Si–Si(lateral)–Si angle, which causes the disorder. The lengths of the Si–O bonds are consistent with the literature data, with an average value of 1.6 Å.[26,33,35] As shown in Fig. 4C, there are C–H···π interactions between toluene molecules and phenyl substituents from one layer (blue) and second layer of **1** (green).

In the case of **1**, due to the high similarity of the flank substituents, the mixture of the geometrical isomers is cumbersome for separation. That is why **1** was applied as an isomeric mixture for further modifications of the inorganic core. Herein, **1** was used to obtain **2**–**4** double-decker silsesquioxanes *via* hydrosilylation reactions. Those reactions were conducted on hydroxyalkyl-substituted alkenes not blocked with TMS or by using epoxides, thus avoiding the stage of deprotection of the blocking group.[37–40]

The syntheses of difunctionalized by hydroxyalkyl substituents double-decker silsesquioxanes are depicted with Scheme 1. In general, all derivatives were synthesized in the reaction between **1** and allyl alcohol (**A**; in the case of **2**), ethylene glycol vinyl ether (**B**; **3**), and 3-allyloxy-1,2-propanediol (**C**; **4**) (Fig. 2), respectively, using a 1 : 5 molar ratio, in anhydrous toluene at 95 °C, under dinitrogen atmosphere, in the presence of Karstedt catalyst.

It is worth mentioning that in these reactions, 2.5 equivalents of alcohol per one lateral silicon atom were used, which was a breaking point. The applied excess of alcohol causes no *O*-silylation by-products. Moreover, this synthetic strategy does

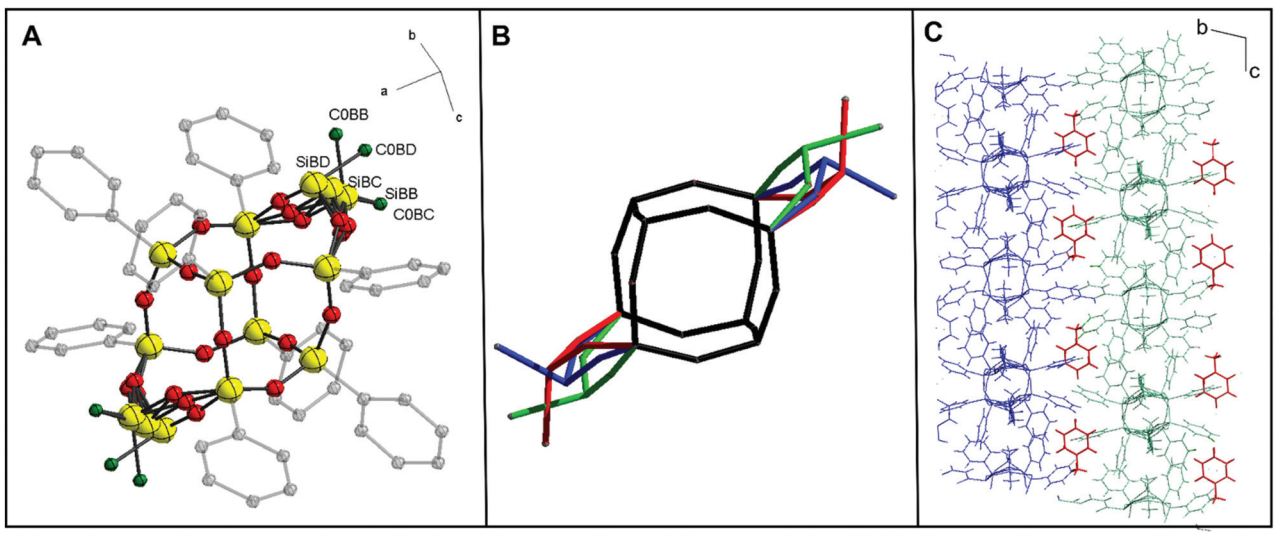

Fig. 4 (A) Molecular structure of *trans*-**1**·C_7H_8, illustrating disordered "lateral" part of the molecule. Color code: C (grey), Si (yellow), O (red). Hydrogen atoms are mitted for clarity. Displacement ellipsoids (for Si and O atoms) are drawn at 50% probability. (B) Schematic representation of three possible conformations. (C) A fragment of the crystal packing.

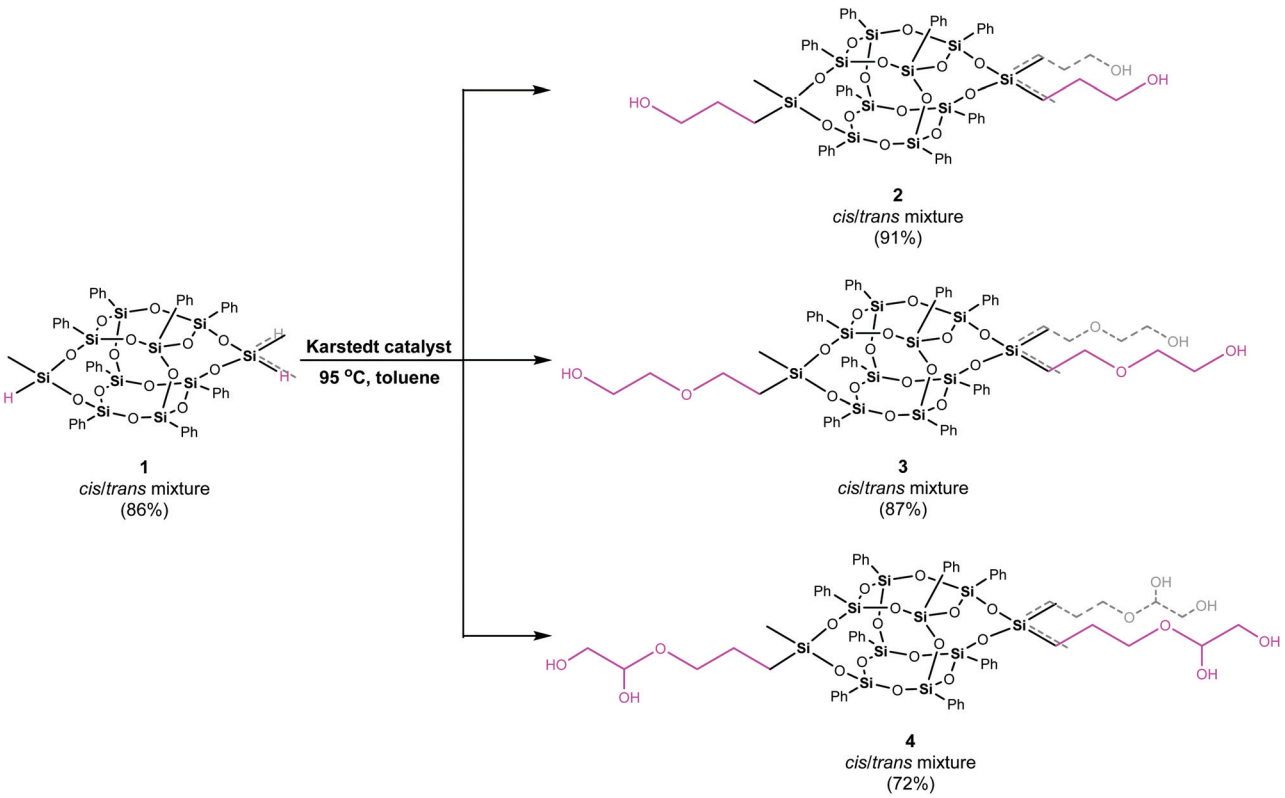

Scheme 1 Synthesis of **2–4**.

not work for unsaturated amines. It was observed that the dehydrogenative silylation occurs for them.

Before the first hydroxyalkyl double-decker silsesquioxane derivative was characterized by physicochemical methods, an uncomplicated and effective separation of the two geometric isomers was carried out (Scheme 2). The crude product was dried and recrystallized in methanol in the first step.

The precipitate did not completely dissolve in the alcohol, and it was confirmed that the *trans* isomer remained in the solid. Next, the filtrate was concentrated using a rotary evaporator to an oil. Hexane was then added to the oil, causing precipitation of the additional amount of *trans* isomer. Finally, the remaining filtrate was concentrated again to oil, and the oil was analyzed. The analysis showed the presence of the *cis* isomer and traces of unreacted functionalized alcohol. An analogous separation strategy can be applied to all derivatives described in this paper. The omission of purification by chromatographic methods is an advantage of using the above-mentioned fractional crystallization.

Fractional crystallization of **2** led to pure *trans*-**2** and the *cis*/*trans* mixture. The *trans*-**2** crystallizes in an orthorhombic system ($P2_12_12_1$ space group; Fig. 5A). The Si–O bond lengths are in the ranges of 1.59–1.63 Å (average value: 1.61 Å), which stays in agreement with the previously reported double-decker silsesquioxane-type structures.[23,24,27] The pseudo-torsion angle C–Si–Si–C (177°) confirms the formation of the *trans*-**2** regioisomer. The Si–Me distances in the "lateral" fragment equal 1.796(2) Å (SiA–C0A) and 1.859(3) Å (SiB–C0B), which is within the length range for already reported systems.[27,33,35] *Trans*-**2** molecules are involved with the strong O–H···O interactions with each other (D···A distances: 3.08(6), 2.80(3), 2.65(4), 2.65(4) Å), which results in the formation of a hydrogen-bonded polymer (Fig. 5B).

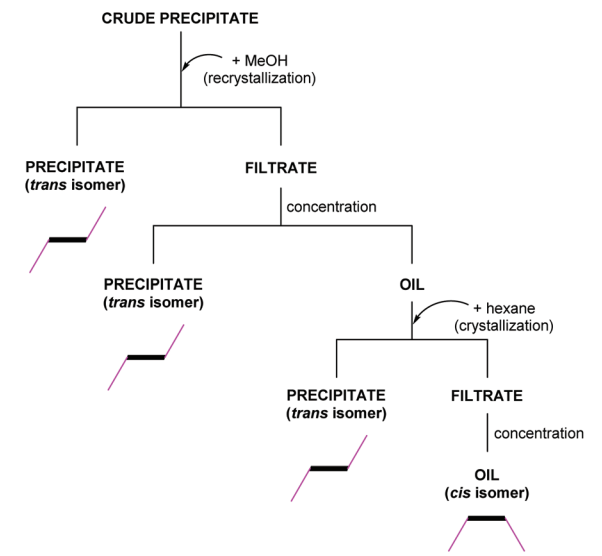

Scheme 2 Flow chart of the fractional crystallization leading to the separation of geometrical isomers.

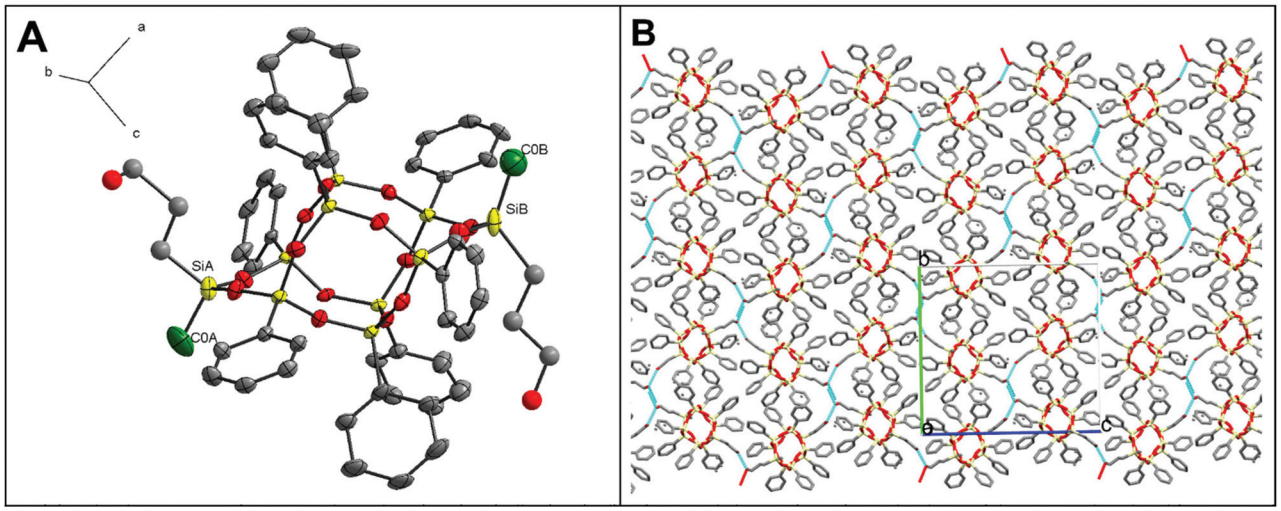

Fig. 5 (A) Molecular structure of *trans*-**2**. Color code: C (grey), Si (yellow), O (red), C from methyl group (green). For the clarity of the picture, disordered fragments of molecule and hydrogen atoms are omitted. All displacement ellipsoids are drawn at 30% probability. Hydroxyalkyl fragments are represented using "ball and stick" (radius 0.3 Å) style. (B) Fragments of crystal packing with hydrogen interactions are marked with blue dots.

Furthermore, the structure of **2** was unambiguously confirmed by multinuclear (^{1}H, ^{13}C, ^{29}Si) NMR spectroscopy, infrared spectroscopy, and high-resolution mass spectrometry. The chemical shifts of ^{29}Si NMR signals were within the expected region for phenyl-substituted closed double-decker silsesquioxane at δ = −78.03, −78.74, and −79.11 ppm for *cis*-**2**, and at −78.59 and −79.56 ppm for *trans*-**2** isomer.

In turn, chemical shifts of the lateral Si nuclei are localized at δ = −17.23 and −17.41 ppm for *cis* and *trans* form, respectively. Furthermore, the characteristic multiplets in the aromatic and alkyl regions in the ^{1}H NMR spectrum indicated the phenyls bounded to Si atoms forming a closed inorganic framework and organic side arms attached to flank silicon nuclei (ESI, Fig. S6†). Additionally, in the FTIR spectrum of **2**, the Si–O–Si stretching gave strong absorption at 1132 cm^{-1}, whereas the presence of hydroxyl groups was observed at 3435 cm^{-1}. The mass spectrum {HRMS (ESI$^+$, TOF/CH_3Cl): *m*/*z* (%): 1292.19 (calcd 1292.15 $[M + Na]^+$)} confirmed the formation of a closed frame structure composed of eight silicon atoms with attached phenyl groups and two silicon atoms in the lateral positions containing terminal hydroxypropyl sidechains and methyl groups.

Since silsesquioxane **2** could not be separated in the form of a crystalline *cis* derivative, it was decided to further modify the organic arm attached to lateral silicon atoms of the inorganic core. The idea of this object was that in the resulting **3**, introducing an additional ether oxygen atom can force the other weak interactions in the crystal lattice. This simple trick made it possible to isolate the *trans*-**3** and *cis*-**3** stereoisomers of double-decker silsesquioxane species in the monocrystalline forms. Their structures were confirmed *via* complex X-ray analyses (see ESI, Tables S3 and S4†). A view of two isomers is presented in Fig. 6. In the case of *cis*-**3**, two solvates were

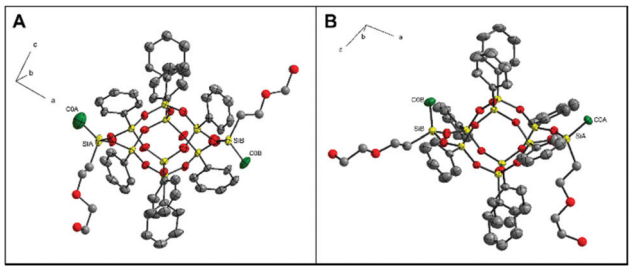

Fig. 6 (A) Molecular structure of *trans*-**3**, and (B) *cis*-**3^2** (room-temperature phase). Color code: C (grey), Si (yellow), O (red), methyl group (green). Hydrogen atoms and disorder of $Si(CH_3)(CH_2CH_2OCH_2CH_2OH)$ fragments in *trans*-**3** and *cis*-**3^2** are omitted for clarity. All displacement ellipsoids are draw at 30% probability. Hydroxyalkyl fragments are represented using "ball and stick" (radius 0.3 Å) style.

obtained: *cis*-**3**·$(CHCl_3)$·0.25(C_2H_5OH) (*cis*-**3^3**, ESI, Fig. S25†) with trichloromethane and ethanol, and *cis*-**3**·0.5(CH_3OH) (*cis*-**3^1**, ESI, Fig. S25†). Both possess the same space group (triclinic, $P\bar{1}$ at 100 K) with an ordered double-decker silsesquioxane core of C_1 symmetry. In both solvates, methyl groups attached to silicon atoms point towards the same direction with a small C0A–SiA–SiB–C0B torsion angles of −3.5° in *cis*-**3^1** (−5° in *cis*-**3^3**), confirming the presence of pure *cis* isomer (Fig. 6B). Si–O skeletons are rigid and adopt almost identical molecular conformation with geometry characteristic of other phenyl-substituted double-decker silsesquioxanes.[35] At 100 K, in *cis*-**3^1**, both side chains are disordered over two inequivalent positions with 0.5/0.5 and 0.6/0.4 occupancy. Van der Waals forces solely design the long-range crystal architecture. Therefore, with increasing temperature (*cis*-**3**·0.5(CH_3OH) (*cis*-**3^2**, ESI, Table S4†), molecular dynamic comes into play and modifies the crystal structure. Around 220 K, global symmetry

grows to monoclinic ($C2/m$), double-decker silsesquioxane adopts C_s symmetry, and the C0A–Si0A–Si0B–C0B torsion angle is reduced to 0°. Both side chains are disordered due to the mirror plane within two equivalent positions. The dielectric relaxation process observed around 220 K confirms the changes in the disorder of side chains (the details concerning the dielectric analysis are presented in ESI, Fig. S26 and S27†). Additionally, the crystal is characterized by high temperature-induced dynamics, which manifests in large values of atoms' displacement parameters.

The presence of trichloromethane stabilizes the side chains in the crystal structure of *cis*-**3**^{3}. Solvents aggregate in (a,c) layers and act as spacers between double-decker silsesquioxane molecules. In *cis*-**3**^{3}, the *b* lattice parameter of 14.27 Å is remarkably longer than 13.95 Å in *cis*-**3**^{1}. This affects both, the distances between molecules and the nature of interactions between them. One hydroxyl group is involved in O–H···Cl interactions (with O···Cl approx. 3.85 Å), whereas the other acts as a donor in the interchain O–H···O hydrogen bond (O···O distance of 2.90 Å) forming polymeric architectures extending towards [110] direction. Fig. 7 shows the crystal packing (without solvates) of *cis*-**3**^{2} with a highlighted polymeric configuration.

In the case of the *trans*-**3** (Fig. 6A), even though the crystals were obtained by slow evaporation from the methanol/toluene mixture, this structure does not form a solvate. Based on the crystallographic data of the analogous compounds (*e.g.*, *trans*-**1**, and others published previously, CSD ref. codes: BEHPOV, NIWLAJ, NODWUA, TASBAT, TIYVAB, TIYVEF, UFEMAW, XETWUR[5,27–29,33,35]), it can be suspected that the *trans* isomer possesses C_i symmetry; however, it crystallizes in the non-centrosymmetric $P2_12_12_1$ space group, like *trans*-**2**. Both Si(CH$_3$)(CH$_2$CH$_2$OCH$_2$CH$_2$OH) fragments were found to be disordered and were refined in two positions each, with site occupation factors equal to 0.7 and 0.3. As a result, some of the molecules in the crystal are rotated 180° compared to others. Therefore, for structure clarity, these groups/atoms are omitted in Fig. 6A. Typically for *trans* geometry, two methyl groups attached to lateral silicon atoms point differently. The torsion angle between C0A–SiA–SiB–C0B is −175°. The angle distortion from ideal 180°, which was noted for these types of structures,[27,33,35] may result from the presence of relatively long alkyl substituents. The overlay of Si–O skeletons (along with methyl groups) for *cis*-**3**^{1} and *trans*-**3** isomers is shown in Fig. 8.

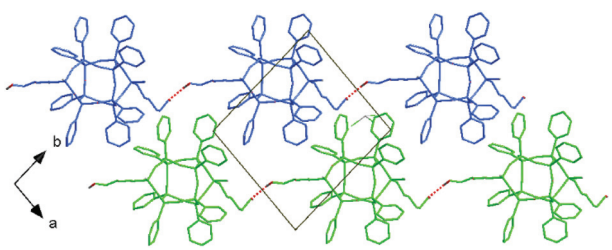

Fig. 7 Crystal packing of *cis*-**3**^{2} with the hydrogen-bonded polymeric architecture. Chains of *cis*-**3**^{2} propagate along the [110] direction.

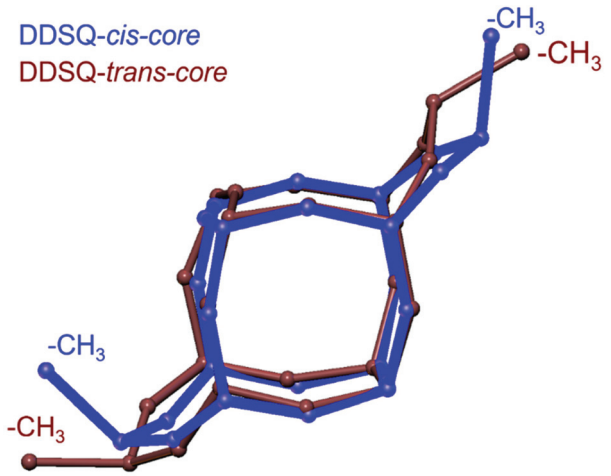

Fig. 8 Overlay of *cis*-**3**^{1} (dark-blue) and *trans*-**3** (brown) isomers' cores. The major occupied atoms were selected for the *trans*-**3** model. The atoms of the *cis*-**3**:*trans*-**3** structures were superimposed as follows: Si1:Si3, Si1(+*x*, 1 − *y*, +*z*), Si2:Si5, O4:O16, O1:O9, O3:O14, Si4:Si2.

Similarly to **2**, for **3**, in the solution sets of assigned to the Si nuclei chemical shifts at δ = −20.05 (Si–Me), −77.45 (*Si*–O–Si–Ph), −78.88, −78.94 (Si–O–*Si*–Ph), and −79.26 ppm (*Si*–O–Si–Ph) for *cis*-**3**, and at −19.55 (Si–Me), −78.59 (*Si*–O–Si–Ph), −79.60 (Si–O–*Si*–Ph) ppm for isomer *trans*-**3** were observed. The HR-MS spectrum {HRMS (ESI$^+$, TOF/CH$_3$Cl): *m*/*z* (%): 1352.21 (calcd 1352.18 [M + Na]$^+$)} also confirmed difunctionalized double-decker silsesquioxane framework (Fig. 1, A) possessing –CH$_2$CH$_2$OCH$_2$CH$_2$OH side arms.

Another modification of the side arms by 3-allyloxy-1,2-propanediol did not lead to the crystallization of further derivatives. Moreover, the spectroscopic characterization of **4** in solution is much more demanding. Due to a chiral carbon atom in organic side arms attached to lateral Si nuclei, the ^{1}H NMR spectra manifest a diastereoisotopic effect. The protons of the methylene group are not equivalent (see signals 7a and 7b in Fig. S18†) due to their vicinity to the stereogenic center. Therefore, it was feasible to observe the separation of their signals. Signals assigned to the Si nuclei have chemical shifts at δ = −78.64 and −79.57 ppm match to Si–O–*Si*–Ph and *Si*–O–Si–Ph for *trans*-**4**, whereas a chemical shift of Si–Me is observed at δ = −17.52 ppm, which confirms the presence of pure *trans* isomer. Chemical shifts at δ = −78.63 (Si–O–*Si*–Ph), −79.44 (*Si*–O–Si–Ph) −79.69 (Si–O–*Si*–Ph), 17.53 (*Si*–Me) correspond to *cis* isomer. In turn, the mass spectrum {HRMS (ESI$^+$, TOF/CH$_3$Cl): *m*/*z* (%): 1439.24 (calcd 1439.22 [M + Na]$^+$)} confirmed the formation of a A-type (Fig. 1, A) double-decker silsesquioxane structure.

4. Conclusions

This work describes a crucial issue related to the preparation of difunctionalized double-decker silsesquioxane derivatives,

which are routinely obtained in the form of a mixture of *cis* and *trans* geometric isomers. A problem often highlighted in the literature is that if the authors describe attempts to separate the mixture, isolating the *trans* isomer in a crystalline form is usually possible. However, the *cis* remains in the difficult to separate mixture of the products. Additionally, it is also in vain to look for the reports regarding the crystal structures of the *cis* double-decker silsesquioxane forms. The present work shows new synthetic strategies for obtaining well-defined *cis* and *trans* isomers containing hydroxyalkyl lateral arms attached to siloxane core. In this manner, we have proof that the modification of the organic arm attached to lateral silicon atoms of the inorganic core by introducing an additional ether oxygen atom can force the other weak interactions in the crystal lattice, resulting in the successful isolation of two stereoisomers in the monocrystalline forms. On the one hand, such derivatives have never been reported. On the other, presented effective protocols can be applied in the further modifications of the double-decker silsesquioxanes leading to *cis* isomers isolation, so few are described in the literature. We are currently exploring further reactions of the resulting hydroxyalkyl derivatives, which may shed more light on creating attractive hybrid materials in various applications, including biomaterials. Investigations along these lines are currently underway.

Conflicts of interest

There are no conflicts to declare.

Acknowledgements

This work was financially supported by the National Science Centre, Poland (Grant No. 2020/39/B/ST4/00910). Furthermore, the authors would like to express their gratitude to Dr Anna Piecha-Bisiorek, D.Sc. from the Faculty of Chemistry, University of Wrocław, Poland, for her cooperation on dielectric studies and to Prof. Tadeusz Lis for his expertise in the X-ray analysis.

References

1 K. Yoshida, T. Hattori, N. Ootake, R. Tanaka and H. Matsumoto, Silsesquioxane-Based Polymers: Synthesis of Phenylsilsesquioxanes with Double-Decker Structure and Their Polymers, in *Silicon Based Polymers*, ed. F. Ganachaud, S. Boileau and B. Boury, Springer, Dordrecht, 2008, pp. 205–211.

2 J. Duszczak, K. Mituła, A. Santiago-Portillo, L. Soumoy, M. Rzonsowska, R. Januszewski, L. Fusaro, C. Aprile and B. Dudziec, Double-Decker Silsesquioxanes Self-Assembled in One-Dimensional Coordination Polymeric Nanofibers with Emission Properties, *ACS Appl. Mater. Interfaces*, 2021, **13**, 22806–22818.

3 R. Sodkhomkhum and V. Ervithayasuporn, Synthesis of Poly (Siloxane/Double-Decker Silsesquioxane) via Dehydrocarbonative Condensation Reaction and Its Functionalization, *Polymer*, 2016, **86**, 113–119.

4 P. Żak, L. Delaude, B. Dudziec and B. Marciniec, N-Heterocyclic Carbene-Based Ruthenium-Hydride Catalysts for the Synthesis of Unsymmetrically Functionalized Double-Decker Silsesquioxanes, *Chem. Commun.*, 2018, **54**, 4306–4309.

5 H.-L. Au-Yeung, S. Y.-L. Leung and V. W.-W. Yam, Supramolecular Assemblies of Dinuclear Alkynylplatinum(II) Terpyridine Complexes with Double-Decker Silsesquioxane Nano-Cores: The Role of Isomerism in Constructing Nano-Structures, *Chem. Commun.*, 2018, **54**, 4128–4131.

6 J. Guan, K. Tomobe, I. Madu, T. Goodson, III, K. Makhal, M. T. Trinh, S. C. Rand, N. Yodsin, S. Jungsuttiwong and R. M. Laine, Photophysical Properties of Functionalized Double Decker Phenylsilsesquioxane Macromonomers: [PhSiO1.5]8[OSiMe2]2 and [PhSiO1.5]8[O0.5SiMe3]4. Cage-Centered Lowest Unoccupied Molecular Orbitals Form Even When Two Cage Edge Bridges Are Removed, Verified By Modeling and Ultrafast Magnetic Light Scattering Experiments, *Macromolecules*, 2019, **52**, 7413–7422.

7 J. Guan, Z. Sun, R. Ansari, Y. Liu, A. Endo, M. Unno, A. Ouali, S. Mahbub, J. C. Furgal, N. Yodsin, S. Jungsuttiwong, D. Hashemi, J. Kieffer and R. M. Laine, Conjugated Copolymers That Shouldn't Be, *Angew. Chem., Int. Ed.*, 2021, **60**, 11115–11119.

8 B. Zhao, H. Ding, S. Xu and S. Zheng, Organic-Inorganic Segmented Polyurethanes Simultaneously Having Shape Recovery and Self-Healing Properties, *ACS Appl. Polym. Mater.*, 2019, **1**, 3174–3184.

9 M. Rzonsowska, K. Mituła, J. Duszczak, M. Kasperkowiak, R. Januszewski, A. Grześkiewicz, M. Kubicki, D. Głowacka and B. Dudziec, Unexpected and frustrating transformations of double-decker silsesquioxanes, *Inorg. Chem. Front.*, 2022, **9**, 379–390.

10 J. Guan, J. J. R. Arias, K. Tomobe, R. Ansari, M. de F. V. Marques, A. Rebane, S. Mahbub, J. C. Furgal, N. Yodsin, S. Jungsuttiwong, D. Hashemi and J. Kieffer, Unconventional conjugation via vinylMeSi(O-)2siloxane bridges may imbue semiconductiong properties in [vinyl (Me)SiO(PhSiO1.5)8OSi(Me)vinyl-Ar] double-decker copolymers, *ACS Appl. Polym. Mater.*, 2020, **2**, 3894–3907.

11 B. Zhao, K. Wei, L. Wang and S. Zheng, Poly(hydroxy urethane)s with double decker silsesquioxanes in the main chains: Synthesis, shape recovery, and reprocessing properties, *Macromolecules*, 2020, **53**, 434–444.

12 Y. Liu, N. Takeda, A. Ouali and M. Unno, Synthesis, characterization, and functionalization of tetrafunctional double-decker siloxanes, *Inorg. Chem.*, 2019, **58**, 4093–4098.

13 Y. Liu, M. Kigure, K. Koizumi, N. Takeda, M. Unno and A. Ouali, Synthesis of tetrachloro, tetraiodo, and tetraazido double-decker siloxanes, *Inorg. Chem.*, 2020, **59**, 15478–15486.

14 T. Uchida, Y. Egawa, T. Adachi, N. Oguri, M. Kobayashi, T. Kudo, N. Takeda, M. Unno and R. Tanaka, Synthesis,

structures, and thermal properties of symmetric and Janus "latern cage" siloxanes, *Chem. – Eur. J.*, 2019, **25**, 1683–1686.

15 B.-D. Barry, J. E. Dannatt, A. K. King, A. Lee and R. E. Maleczka, A general diversity oriented synthesis of asymmetric double-decker shaped silsesquioxanes, *Chem. Commun.*, 2019, **55**, 8623–8626.

16 J. Duszczak, K. Mituła, R. Januszewski, P. Żak, B. Dudziec and M. Marciniec, Highly efficient route for the synthesis of a novel generation of tetraorganofunctional double-decker type of silsesquioxanes, *ChemCatChem*, 2019, **11**, 1086–1091.

17 Y. Du and H. Liu, Cage-like silsesquioxanes-based hybrid materials, *Dalton Trans.*, 2020, **49**, 5396–5405.

18 M. Soldatov and H. Liu, Hybrid porous polymers based on cage-like organosiloxanes: synthesis, properties and applications, *Prog. Polym. Sci.*, 2021, **119**, 101419.

19 W. Mingyue, C. Hong, K. S. Joshy and W. Fuke, Progress in the synthesis of bifunctionalized polyhedral oligomeric silsesquioxane, *Polymers*, 2019, **11**, 2098.

20 B. Dudziec and M. Marciniec, Double-decker silsesquioxanes: current chemistry and applications, *Curr. Org. Chem.*, 2017, **21**, 2794–2813.

21 M. A. Hoque, Y. Kakihana, S. Shinke and Y. Kawakami, Polysiloxanes with Periodically Distributed Isomeric Double-Decker Silsesquioxane in the Main Chain, *Macromolecules*, 2009, **42**, 3309–3315.

22 V. Ervithayasuporn, R. Sodkhomkhum, T. Teerawatananond, C. Phurat, P. Phinyocheep, E. Somsook and T. Osotchan, Unprecedented formation of *cis*- and *trans*-di[(3-chloropropyl)isopropoxysilyl]-bridged double-decker octaphenylsilsesquioxanes, *Eur. J. Inorg. Chem.*, 2013, 3292–3296.

23 V. Ervithayasuporn, X. Wang and Y. Kawakami, Synthesis and characterization of highly pure-azido-functionalized polyhedral oligomeric silsesquioxanes (POSS), *Chem. Commun.*, 2009, **34**, 5130–5132.

24 J. Jung, H. J. C. Furgal, T. Goodson III, T. Mizumo, M. Schwartz, K. Chou, J.-F. Vonet and R. M. Laine, 3-D Molecular Mixtures of Catalytically Functionalized $[vinylSiO_{1.5}]_{10}$/$[vinylSiO_{1.5}]_{12}$. Photophysical Characterization of Second Generation Derivatives, *Chem. Mater.*, 2012, **24**, 1883–1895.

25 M. Janeta, Ł. John, J. Ejfler and S. Szafert, Novel organic-inorganic hybrids based on T8 and T10 silsesquioxanes: synthesis, cage-rearrangement and properties, *RSC Adv.*, 2015, **5**, 72340–72351.

26 Y. Morimoto, K. Watanabe, N. Ootake, J. Inagaki, K. Yoshida and K. Ohguma, Silsesquioxane derivative and production process for the same, *US Pat*, 7449539B2, 2008.

27 L. M. J. Moore, J. J. Zavala, J. T. Lamb, J. T. Reams, G. R. Yandek, A. J. Guenthner, T. S. Haddad and K. B. Ghiassi, Bis-phenylethynyl polyhedral oligomeric silsesquioxanes: new high-temperature, processable thermosetting materials, *RSC Adv.*, 2018, **8**, 27400–27405.

28 D. F. Vogelsang, J. E. Dannatt, B. W. Schoen, R. E. Maleczka, Jr. and A. Lee, Phase Behavior of *cis–trans* Mixtures of Double-Decker Shaped Silsesquioxanes for Processability Enhancement, *ACS Appl. Nano Mater.*, 2019, **2**, 1223–1231.

29 P. Żak, B. Dudziec, M. Kubicki and B. Marciniec, Silylative Coupling versus Metathesis—Efficient Methods for the Synthesis of Difunctionalized Double-Decker Silsesquioxane Derivatives, *Chem. – Eur. J.*, 2014, **20**, 9387–9393.

30 V. Vij, G. Yandek, S. Ramirez, J. M. Mabry and T. S. Haddad, *Polym. Prepr.*, 2012, **53**, 513.

31 K. Wei, L. Wang and S. Zheng, Organic-inorganic polyurethanes with 3,13-dihydroxyoctaphenyl double-decker silsesquioxane chain extender, *Polym. Chem.*, 2013, **4**, 1491–1501.

32 K. Koppe, J. Eichhorn, B. Jeffery, A. Davis, W. Mitchell, P. Miskiewicz and T. Nonaka, WO 2020/182636A1, 2020.

33 M. Walczak, R. Januszewski, M. Majchrzak, M. Kubicki, B. Dudziec and B. Marciniec, Unusual *cis* and *trans* architecture of dihydrofunctional double-decker shaped silsesquioxane and synthesis of its ethyl bridged π-conjugated arene derivatives, *New J. Chem.*, 2017, **41**, 3290–3296.

34 B. W. Schoen, D. Holmes and A. Lee, Identification and quantification of cis and *trans* isomers in aminophenyl double-decker silsesquioxanes using ^{1}H-^{29}Si gHMBC NMR, *Magn. Reson. Chem.*, 2013, **51**, 490–496.

35 T. Tanaka, Y. Hasegawa, T. Kawamori, R. Kunthom, N. Takeda and M. Unno, Synthesis of Double-Decker Silsesquioxanes from Substituted Difluorosilane, *Organometallics*, 2019, **38**, 743–747.

36 E. Arunan and H. S. Gutowsky, The rotational spectrum, structure and dynamics of a benzene dimer, *J. Chem. Phys.*, 1993, **98**, 4294–4296.

37 Z. Niu, D. Tian, L. Yan, X. Ma, C. Zhang and X. Hou, Synthesis of 3,13-diglycidyloxypropyloctaphenyl double-decker polyhedral oligomeric silsesquioxane and the thermal reaction properties with thermosetting phenol-formaldehyde resin, *J. Appl. Polym. Sci.*, 2020, **137**, 49376–49386.

38 L. Wang, C. Zhang and S. Zheng, Organic-inorganic poly (hydroxyether of bisphenol A) copolymers with double-decker silsesquioxane in the main chains, *J. Mater. Chem.*, 2011, **21**, 19344–19352.

39 J. Cao, H. Fan, B.-G. Li and S. Zhu, Synthesis and evaluation of double-decker silsesquioxanes as modifying agent for epoxy resin, *Polymer*, 2017, **124**, 157–167.

40 C.-H. Lin, W.-B. Chen, W.-T. Whang and C.-H. Chen, Characteristics of Thermosetting Polymer Nanocomposites: Siloxane-Imide-Containing Benzoxazine with Silsesquioxane Epoxy Resins, *Polymers*, 2020, **12**, 2510.

41 S.-E. Zhu, W.-J. Yang, Y. Zhou, W.-H. Pan, C.-X. Wei, A. C. Y. Yuen, T. B. Y. Chen, G. H. Yeoh, H.-D. Lu and W. Yang, *Chem. Eng. J.*, 2022, **442**, 136367.

42 A. A. Balandin, *Nat. Mater.*, 2011, **10**, 569–581.

43 L. Liu, M. Zhu, Z. Ma, X. Xu, J. Dai, Y. Yu, S. Mohsen Seraji, H. Wang and P. Song, *Chem. Eng. J.*, 2022, **440**, 135645.

